

Color Variability of the Blazar AO 0235+16*

V. A. Hagen-Thorn,¹ V. M. Larionov,^{1,2} C. M. Raiteri,³ E. I. Hagen-Thorn,^{2,1}
A. V. Shapiro,¹ A. A. Arkharov,² L. O. Takalo,⁴ and A. Sillanpää⁴

¹*Sobolev Astronomical Institute, St. Petersburg State University*

²*Main (Pulkovo) Astronomical Observatory, Russian Academy of Sciences*

³*INAF—Osservatorio Astronomico di Torino*

⁴*Tuorla Observatory, University of Turku*

Multicolor (UBVRIJHK) observations of the blazar AO 0235+16 are analyzed. The light curves were compiled at the Turin Observatory from literature data and the results of observations obtained in the framework of the WEBT program (<http://www.to.astro/blazars/webt/>). The color variability of the blazar was studied in eight time intervals with a sufficient number of multicolor optical observations; JHK data are available for only one of these. The spectral energy distribution (SED) of the variable component remained constant within each interval, but varied strongly from one interval to another. After correction for dust absorption, the SED can be represented by a power law in all cases, providing evidence for a synchrotron nature of the variable component. We show that the variability at both optical and IR wavelengths is associated with the same variable source.

1. INTRODUCTION

AO 0235+16 has recently been one of the most intensively studied BL Lac objects [1–4]. Raiteri et al. [1–3] present a virtually complete bibliography with a description of the object's parameters, and we will not reproduce them here. We note only that the variability amplitude of AO 0235+16 reaches 5^m , and its observed color is anomalously red for blazars. An absorption system with $z = 0.524$ is seen in the spectrum of AO 0235+16 ($z_{\text{em}} = 0.94$). Junkkarinen et al. [4] showed that the region responsible for this absorption system lines contains a large amount of dust that leads to the strong reddening. Therefore, all estimates of spectral indices and other parameters obtained before [4] should be revised. In particular, this is true of the data of Hagen-Thorn et al. [5] (although their conclusion concerning the large color variations of the sources, which are responsible for variability with a characteristic time scale of about a year, remains valid). The color

*Astronomy Reports, 2007, Vol. 51, No. 11, pp. 882–890. ©Pleiades Publishing, Ltd., 2007

variability of AO 0235+16 is discussed in [3]. However, we believe that a more detailed analysis is needed, using the technique described in [6], which has been applied to the color variability of blazars in many studies (see, for example, [7, 8]).

2. OBSERVATIONS AND TECHNIQUE OF THE ANALYSIS

Here, we use the $UBVRI$ (optical) and JHK (near-IR) light curves compiled by C.M. Raitieri at the Torino Observatory, based on published data and data obtained as a result of combining and comparing observations taken as part of the WEBT Program (Whole Earth Blazar Telescope; <http://www.to.astro/blazars/webt/>), in which the authors take part. Regular IR observations started in 2002; optical data are available since 1975, when the radio source was identified with a star-like object. Figure 1 presents light curves in one optical (R) and one IR (K) band as examples (nightly averaged fluxes are given, which we will also use in our subsequent analysis, thereby eliminating very rapid variability in favor of studying color variations on time scales exceeding a day). We transformed the magnitudes into fluxes using the calibration of Mead et al. [9].

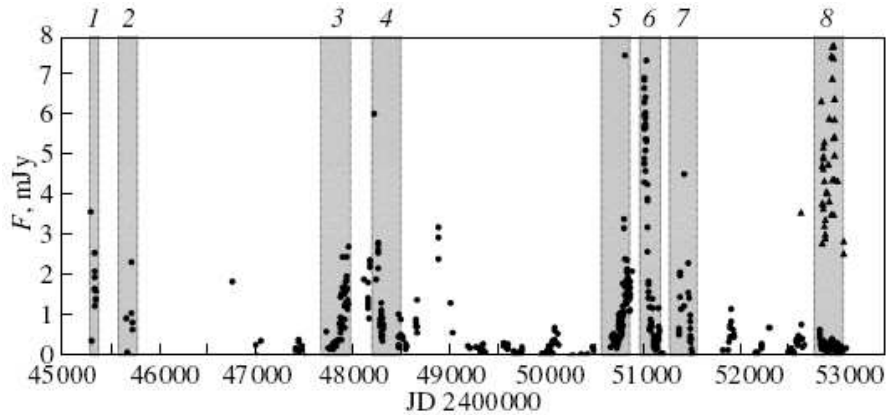


Figure 1: *Light curve of AO 0235+16 in the R (points) and K (triangles) bands. Time intervals within which the color variability was studied are indicated.*

The idea of our technique for analyzing color variability is to construct flux–flux diagrams for pairs of bands (or, to be more precise, the flux density is considered). If the color characteristics of the variable component are unchanged, the points in the diagrams should lie on straight lines, whose slopes yield the ratios of the fluxes of the *variable* component in the bands considered. In this way, multicolor observations of variability can be used to derive the relative spectral energy distribution (SED) of the variable source.

It is convenient to determine the SED of the variable source separately for optical and IR wavelengths. These distributions can then be joined using a flux–flux diagram comparing fluxes in one of the optical and one of IR bands.

The most noteworthy advantage of the method is that obtaining the relative SED of a variable component does not require previous determination of its contribution to the combined observed radiation.

3. THE RESULTS OF THE ANALYSIS OF THE COLOR VARIABILITY

As was shown in our earlier study [5], the color characteristics of the variable component of AO 0235+16 can vary, and rather rapidly. Accordingly, we chose eight time intervals, within which we determined the relative SED of the variable component (the light curves indicate that it is the variable component that determines the photometric behavior of the object in these intervals, whose edges are indicated in Fig. 1). A pairwise comparison of the observed fluxes in different spectral bands indicates that they are related linearly (seen from the fact that the correlation coefficients are close to unity), so that the SED of the variable component within each time interval may be considered as constant. We carried out such comparisons separately for optical and IR wavelengths, selecting R and K as the primary bands.

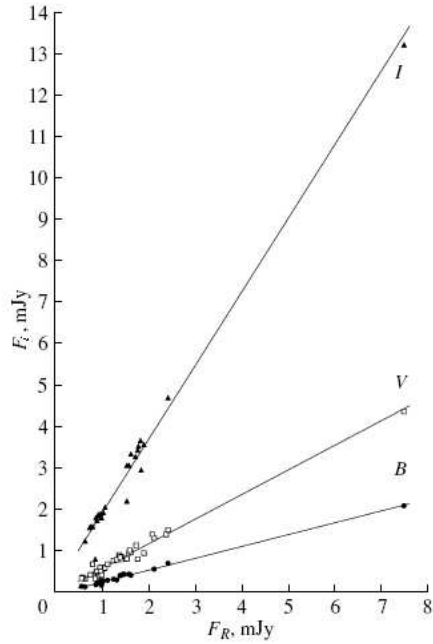


Figure 2: *Flux–flux diagrams for interval 5.*

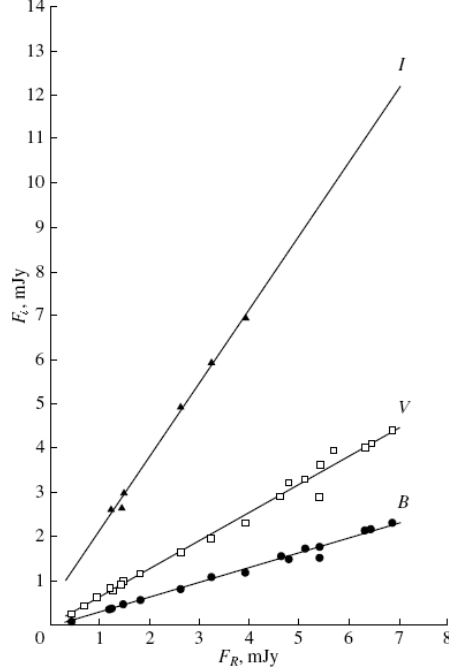


Figure 3: *Flux–flux diagrams for interval 6.*

To avoid overburdening the paper, we will present detailed results for three most interesting intervals, and only final results for the remaining ones. Figures 2–5 present the flux–flux diagrams for intervals 5 (JD 2450600–2450900, 1997–1998), 6 (JD 2451000–2451200, 1998–1999) and 8 (JD 2452800–2453100, 2003).

Figure 6 shows the flux–flux diagram for R and K bands, used to construct joint optical and IR spectrum in interval 8 (the only interval for which there are IR data). The slopes of the lines derived via an orthogonal regression fit [10] (this technique should be used when both compared values display random errors) are presented in the fifth columns of Tables 1–3, along with their 1σ errors. These yield the observed relative SED of the variable component. (The first four columns of these tables present (1) band, (2) logarithm of the corresponding frequency, (3) correlation coefficient, and (4) number of points in the graphs.) An important stage in the analysis is correcting the observed distribution for absorption by intervening dust clouds. This correction is introduced by multiplying the values in the fifth columns of Tables 1–3 by the factor C_{iR} (C_{iK} for IR bands), derived from the absorption data taken from the last column of Table 5 in [2], where all sources of absorption are taken into account in accordance with [4]. The absorption values are presented in the sixth columns of Tables 1–3, and the factors C_{iR} (C_{iK}) in the seventh columns.

The $(F_i/F_R)_{var}^{corr}$ ratios, corrected for absorption, which give the relative SED of the variable component, are presented in the eighth columns of Tables 1–2 and the eighth and ninth columns of

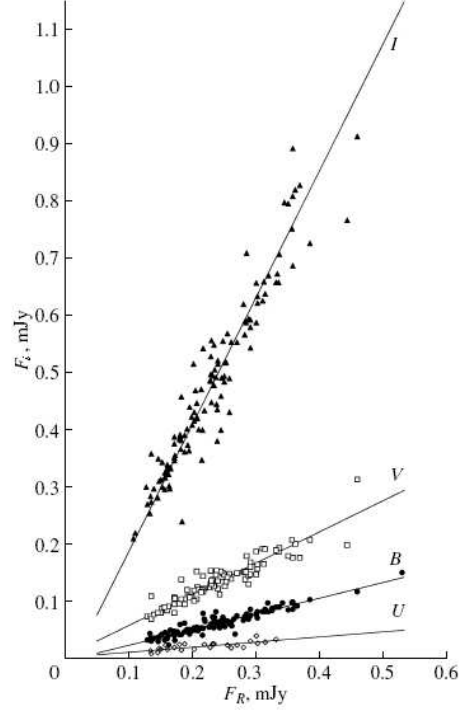


Figure 4: *Flux-flux diagrams for interval 8 at optical wavelengths.*

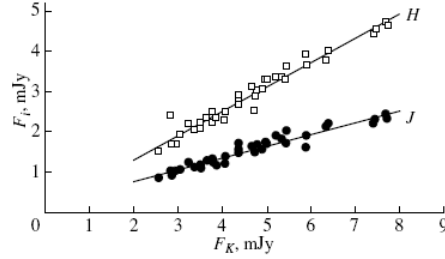


Figure 5: *Flux-flux diagrams for interval 8 at infrared wavelengths.*

Table 3. The last columns of Tables 1–3 contain the logarithms of these ratios, which are plotted against $\log \nu$ in Figs. 7 and 8. Figure 8 separately presents the optical and IR SEDs and the joint SED for the total range from K to U .

Figures 7 and 8 show that the dots lie along straight lines fairly well; i.e., the SED of the variable component follows the power law $F_\nu \sim \nu^\alpha$, where the spectral index α is given by the slopes of the lines in the graphs, which were derived via least-squares fitting. The α values for all eight time intervals are presented along with their 1σ errors in the third column of Table 4 (the second column indicates the interval, the fourth the correlation coefficient between $\log(F_i/F_R)_{var}^{corr}$ and $\log \nu$, and the fifth and sixth are the average and maximum fluxes in the R band). For uniformity, the α value found from the optical data is presented for interval 8. In this interval, the spectral index

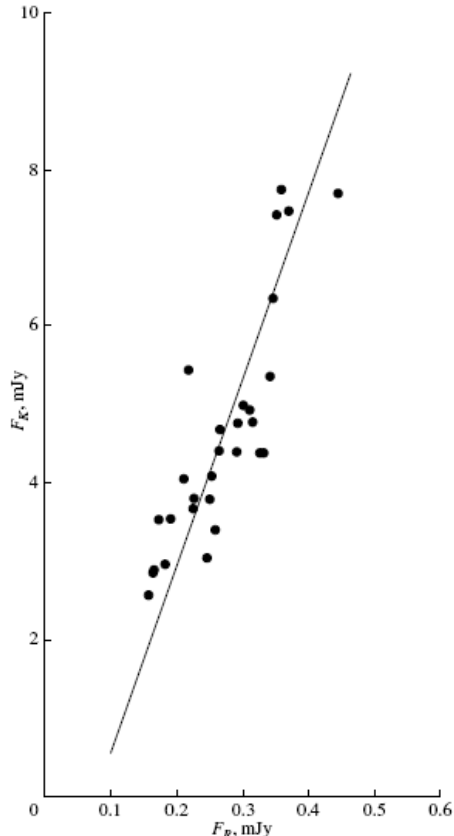


Figure 6: *Flux-flux diagrams for interval 8 and the R and K bands.*

$\alpha = -1.66 \pm 0.12$ was found for the IR wavelengths, with a correlation coefficient of $r = 0.99$, while we find $\alpha = -1.92 \pm 0.05$ with $r = 0.99$ for the joint SED

4. DISCUSSION AND CONCLUSIONS

The power spectrum and high polarization usually observed in AO 0235+16 (for example, according to our unpublished data, it exceeded 30% in December 2006) provide clear evidence for a synchrotron nature for the variable sources responsible for this activity.

We can see from Figs. 2–5 that the lifetimes of the variable sources could be hundreds of days, but apparently do not exceed a year, since the corresponding spectral indices for different seasons differ dramatically (Table 4). This is particularly striking for intervals 5 and 6. Figure 1 indicates that the flux increases in interval 5, while it decreases in interval 6. Unfortunately, a seasonal gap in the optical light curve lies between intervals 5 and 6. One might think that we are dealing here with a single event (Fig. 8 from [1], which presents radio light curves, does not seem to contradict this). However, the spectrum is steeper in interval 5, when the flux increases, than in interval

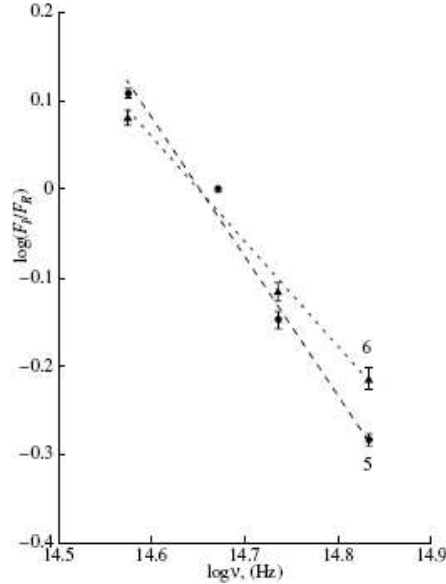


Figure 7: Spectra of variable sources in intervals 5 and 6.

6, when it decreases. Current evolutionary mechanisms for variable sources predict the opposite behavior. Therefore, we conclude that in intervals 5 and 6 different events were observed.

Figure 9 compares the spectral indices with the average values for a given time interval and maximum R flux, according to the data in Table 4. In the first case, a random cloud of points is observed; however, weak ($r = 0.2$) correlation is observed for the maximum flux: harder (flatter) spectra correspond to higher maximum fluxes in an event. Such behavior (expected from general considerations) was already noted by Hagen-Thorn et al. [5] for the blazar OJ 287.

Let us now consider Fig. 8. We can clearly see that there is no discontinuity between the data for the optical and IR wavelengths in the joint SED. The optical spectrum is slightly steeper, possibly indicating a high-frequency cutoff. However, the data for shorter wavelengths (see Fig. 10 in [2]) do not support this possibility. Such a small break in the spectrum could be due to a small underestimation of the absorption (this is quite possible in our case). Taking this into account, as well as the fact that the difference between the optical and IR spectral indices does not exceed the 2σ uncertainties, we suggest that the variability in both spectral regions was associated with the same variable source, and that the joint SED represents the relative SED in time interval 8 over the entire frequency range from K to U. The spectral index ($\alpha = -1.92$) that we have derived is rather common for blazars.

In conclusion, we note that, due to the pronounced differences between the SEDs of the variable component in different time intervals, a comparison of the observed color indices and brightnesses

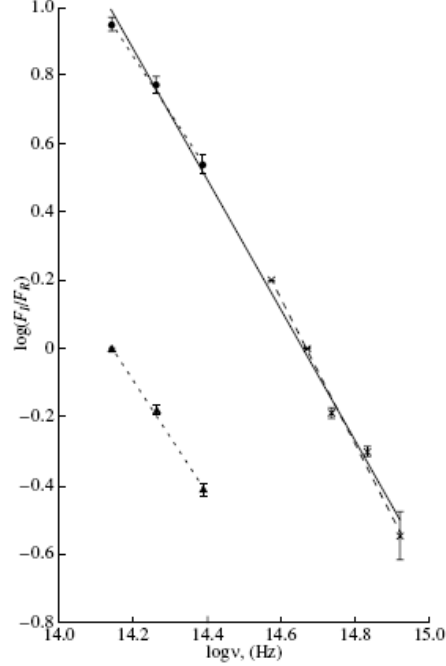


Figure 8: *Spectrum of the variable source in interval 8. The IR (triangles) and optical (crosses) spectra and the “joint” spectrum (points and solid line) are plotted separately.*

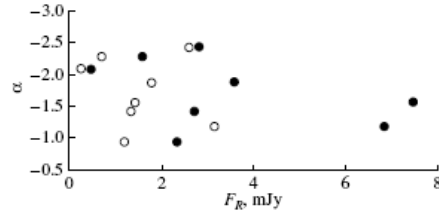


Figure 9: *Comparison of the spectral indices of the variable source at optical wavelengths with the R flux. Open circles correspond to \bar{F}_R , and filled circles to F_R^{max} .*

for the entire set of observational data contains little information. Moreover, such a comparison could lead to the erroneous conclusion that the SED of the variable component varies during an outburst.

ACKNOWLEDGMENTS

This work was supported by the Russian Foundation for Basic Research (project code 05-02-17562). V.A.H.-T. and E.I.H.-T. thank Tuorla Observatory for hospitality. L.O.T. and A.S. are grateful to the Academy of Sciences of Finland, which also supported the study. C.M.R. thanks the Italian Space Agency, which supported this work in the frame of Contract ASI-INAF

I/023/05/0. Observations with the AZT-24 Telescope are made in accordance with an agreement between the Main (Pulkovo) Observatory of the Russian Academy of Sciences and the Rome and Teramo Observatories (Italy).

1. C.M.Raiteri, M.Villata, H.D.Aller, et al., *Astron. and Astrophys.J.*, **377**, 396, 2001.
2. C.M.Raiteri, M.Villata, M.A.Ibrahimov, et al., *Astron. and Astrophys.*, **438**, 39, 2005.
3. C.M.Raiteri, M.Villata, M.Kadler, et al., *Astron. and Astrophys. J.*, **459**, 731, 2006.
4. V.T.Junkkarinen, R.D.Cohen, E.A.Beaver, et al., *Astrophys.J.*, **614**, 658, 2004.
5. V.A.Hagen-Thorn, S.G.Marchenko, and O.V.Mikolaichiuk, *Astrofizika*, **32**, 429, 1990.
6. V.A.Hagen-Thorn and S.G.Marchenko, *Baltic Astronomy*, **8**, 575, 1999.
7. V.A.Hagen-Thorn, *ASP Conf. Ser.*, **350**, 41, 2006.
8. V.A.Hagen-Thorn, V. M. Larionov, N. V. Efimova, et al., *Astron. Zh.* 83, 516 (2006)
9. A.R.J.Mead, K.R.Ballard, P.W.J.L.Brand, et al., *Astron. and Astrophys. Suppl. Ser.* **83**, 183, 1990.
10. A.Wald, *Ann. Math. Stat.* **11**, 284, 1940.
11. V.A.Hagen-Thorn, S.G.Marchenko, L.O.Takalo et al., *Astron. and Astrophys. Suppl. Ser.* **133**, 353, 1990.

Table 1: Results for interval 5 (JD 2450600–2450900, 1997–1998))

Band	$\log \nu$	r_{iR}	n	$(F_i/F_R)_{var}^{obs} \pm 1\sigma$	$A_{i,m}$	C_{iR}	$(F_i/F_R)_{var}^{corr} \pm 1\sigma$	$\log(F_i/F_R)_{var}^{corr} \pm 1\sigma$
B	14.833	0.99	21	0.287 ± 0.005	1.904	1.810	0.519 ± 0.009	-0.284 ± 0.007
V	14.736	0.99	35	0.596 ± 0.013	1.473	1.194	0.711 ± 0.016	-0.148 ± 0.010
R	14.670	-	-	1.000	1.260	1.000	1.000	0.000
I	14.574	0.99	25	1.783 ± 0.022	0.902	0.719	1.282 ± 0.016	0.108 ± 0.005

Table 2: Results for interval 6 (JD 2451000–2451200, 1998–1999))

Band	$\log \nu$	r_{iR}	n	$(F_i/F_R)_{var}^{obs} \pm 1\sigma$	$A_{i,m}$	C_{iR}	$(F_i/F_R)_{var}^{corr} \pm 1\sigma$	$\log(F_i/F_R)_{var}^{corr} \pm 1\sigma$
B	14.833	0.99	16	0.337 ± 0.009	1.904	1.810	0.610 ± 0.016	-0.215 ± 0.012
V	14.736	0.99	20	0.639 ± 0.015	1.473	1.194	0.763 ± 0.018	-0.117 ± 0.010
R	14.670	-	-	1.000	1.260	1.000	1.000	0.000
I	14.574	0.99	6	1.673 ± 0.030	0.902	0.719	1.203 ± 0.022	0.080 ± 0.008

(1) - For the J and H bands, relative to the K band.

Table 3: Results for interval 8 (JD 2452800–2453100, 2003))

Band	$\log \nu$	$r_{iR}(1)$	n	$(F_i/F_R)_{var}^{obs} \pm 1\sigma(1)$	$A_{i,m}$	$C_{iR}(1)$	$(F_i/F_R)_{var}^{corr} \pm 1\sigma(1)$	$(F_i/F_R)_{var}^{corr} \pm 1\sigma$	$\log(F_i/F_R)_{var}^{corr} \pm 1\sigma$
U	14.920	0.77	25	0.089 ± 0.015	2.519	3.188	0.284 ± 0.048	0.284 ± 0.048	-0.547 ± 0.068
B	14.833	0.94	107	0.276 ± 0.009	1.904	1.810	0.500 ± 0.016	0.500 ± 0.016	-0.301 ± 0.014
V	14.736	0.93	89	0.545 ± 0.020	1.473	1.194	0.651 ± 0.024	0.651 ± 0.024	-0.187 ± 0.016
R	14.670	-	-	1.000	1.260	1.000	1.000	1.000	0.000
I	14.574	0.96	122	2.223 ± 0.025	0.902	0.719	1.598 ± 0.018	1.598 ± 0.018	0.204 ± 0.004
K	14.140	0.85	29	24.26 ± 0.100	0.171	0.367	8.903 ± 0.040	-	-
J	14.387	0.97	38	0.298 ± 0.013	0.458	1.302	0.388 ± 0.017	3.454 ± 0.057	0.538 ± 0.007
H	14.262	0.98	38	0.604 ± 0.018	0.275	1.100	0.664 ± 0.020	5.912 ± 0.060	0.772 ± 0.004
K	14.140	-	-	1.000	0.171	1.000	1.000	8.903 ± 0.040	0.950 ± 0.020

Table 4: Spectral index of the variable component for various time intervals

Interval	$\alpha \pm \sigma_\alpha$	r	\overline{F}_R	F_R^{max}
1, JD 2445300-2445400	-1.88 ± 0.26	0.95	1.78	3.59
2, JD 2445600-2445800	-0.94 ± 0.18	0.96	1.19	2.34
3, JD 2447700-2448000	-1.42 ± 0.23	0.95	1.33	2.72
4, JD 2448220-2448350	-2.43 ± 0.23	0.97	2.59	2.82
5, JD 2445600-2445900	-1.56 ± 0.13	0.99	1.43	7.48
6, JD 2451000-2451200	-1.18 ± 0.11	0.98	3.16	6.85
7, JD 2451300-2451600	-2.29 ± 0.59	0.93	0.69	1.58
8, JD 2452800-2453100	-2.09 ± 0.14	0.99	0.25	0.46